Chin. J. Astron. Astrophys. Vol. 8 (2008), **Supplement**, 61–76
(*http://www.chjaa.org*)

Chinese Journal of
Astronomy and
Astrophysics

Cluster of Galaxies: the Largest Multi-Frequency Laboratories for Astro-Particle Physics

Sergio Colafrancesco[1,2,3] ⋆

[1] ASI Science Data Center, ASDC c/o ESRIN, via G. Galilei 00044 Frascati, Italy
[2] Agenzia Spaziale Italiana, Unità Osservazione dell'Universo, viale Liegi 26 00198 Roma, Italy
[3] INAF - Osservatorio Astronomico di Roma, Via Frascati 33, 00040 Monteporzio, Italy

Abstract We discuss the relevance of multi–frequency analysis of galaxy clusters to unveil several issues that are relevant for Cosmology and Astro-Particle Physics of cosmic structures: the nature of Dark Matter, the origin of cosmic rays, the role of magnetic fields and the impact of black holes.

Key words: cosmology: theory — galaxies: clusters

1 INTRODUCTION

Galaxy clusters are the largest, gravitationally bound structures in the universe and are representative systems of the distribution of Large Scale Structures (LSS) in the universe. The description of these cosmic structures is continuously enriching of physical details regarding their matter and field content.

Dark Matter (DM) is the dominant form of matter that create their potential wells: if we consistently take into account the fundamental nature of DM particles,[1] we are inevitably bound to consider the effects of their annihilation (in the case of SUSY DM particles) or their decay (in the case of sterile neutrinos) on the structure and evolution of the cluster atmospheres.

Baryonic material collected in the DM potential wells associated to LSS is likely heated and shocked by large–scale shock waves found in cosmological simulations (see, e.g. Ryu et al. 2003; Pfrommer et al. 2007) which produce a complex distribution of Mach numbers, with shock velocities $V_{\rm shock} \lesssim 250\,{\rm km\ s^{-1}}$ at the intergalactic shocks and $250 \lesssim V_{\rm shock} \lesssim 1000\,{\rm km\ s^{-1}}$ at shocks found inside clusters (see, e.g. Ryu et al. 2003). LSS shock waves have been suggested to exist in large scale filaments (see Bagchi et al. 2002 for the case of the large-scale filament of galaxies ZwCl 2341.1+0000) and in clusters (see Sarazin 2001 for a review). The presence of shock waves with relatively high Mach numbers naively suggest that Fermi-like acceleration might take place in LSS thereby accelerating **cosmic rays** (CRs) that can be efficiently confined especially in galaxy clusters (see e.g. Colafrancesco & Blasi 1998 and references therein).

Radio observations and Magneto-hydrodinamic (MHD) simulations also suggest that large scale **magnetic fields** (of either primordial origin or post-recombination generation, see e.g. Giovannini 2005 for a review) are associated to the distribution of baryonic material collected in LSS potential wells (see e.g. Sigl et al. 2005; Dolag et al. 2004). The seed magnetic field is likely amplified and made turbulent by the coupling of gravitational collapse and MHD processes during the formation of galaxy clusters. Evidence for such wide-scale and turbulent intra-cluster magnetic field is indicated by the diffuse radio synchrotron emission found in many nearby clusters (with typical values $B \sim 0.1 - 2\ \mu$G), by radio relic features in dynamically active clusters (with typical values $B \sim 0.2 - 5\ \mu$G) and by Faraday Rotation measurements

⋆ E-mail: cola@mporzio.astro.it

[1] Viable candidates for the DM are neutralinos (the lightest MSSM particles, see Jungman et al. 1996), sterile neutrinos (the lightest right-handed neutrino, see Shaposhnikov 2007) or even other forms of light DM, see Boyanovsky et al. 2007).

of background and embedded polarized radio sources (with typical values $B \sim 1 - 50\ \mu$G, Carilli & Taylor 2002; Govoni & Feretti 2004).

Very massive DM clumps that collapse at high redshifts ($z \sim 6 - 7$) often contain the most massive **Black Holes** (BHs) at their centers (see, e.g., results from the Millennium simulation, Springel et al. 2005). The AGN descendants of these ancient supermassive BHs are found to be part of the massive galaxies located at the centers of the most massive galaxy clusters we observe at the present epoch. We know, in fact, that massive radio galaxies and blazars are often found in the cores of galaxy clusters (like, e.g., CenA, M87/Virgo, Perseus, A262, A4059) with their radio lobes penetrating the ICM for tens or hundreds of kpcs. It is often observed that the radio jets/lobes end up in approximately spherical **bubbles of relativistic plasma** (likely containing relativistic or mildly-relativistic plasmas) that appear as cavities in the X-ray images of galaxy clusters (see e.g. Birzan et al. 2004) with dimensions ranging from a few kpcs (as in Perseus) to $\sim 100\,$kpc (as in the case of the cluster MS0735–556, McNamara & Nulsen 2007). The combination of high-resolution radio and X-ray images provides the notion that the relativistic plasma found inside the X-ray cavities is indeed connected with the jet/lobe structure of the central AGN and with the history of the ejection mechanisms of non-thermal plasma from the central AGN.

The cores of galaxy clusters which host such non-thermal phenomena (BHs, cavities, high magnetic fields, see Eilek & Owen 2006) are found to be systematically cooler than the outer regions of the clusters with the inner temperature setting at a value $\sim \frac{1}{3} - \frac{1}{2}$ of the outer temperature, usually consistent with the virial expectation (see Peterson & Fabian 2006; McNamara & Nulsen 2007; Bregman 2003 and references therein for recent reviews). It seems that a heating agent of non-gravitational and non-thermal nature – with a heating rate which is able to accomodate itself to the cooling rate of the intra-cluster plasma – is present in the cluster's **cool core** so as to maintain it in a quasi-stationary, warm configuration (Colafrancesco, Dar & DeRujula 2004; Colafrancesco & Marchegiani 2007).

The previous evidence indicates that galaxy clusters – the largest bound structures in the universe – are the largest storage rooms for cosmic material (galaxies, DM, hot thermal plasma, non-thermal and relativistic plasma, BHs, magnetic fields, CRs). In this sense they can be considered as the largest laboratories for Astro Particle Physics in the universe. In such laboratories one can efficiently study some of the most interesting aspects of the astro-particle physics of LSS: the nature of DM, the origin and distribution of CRs, the impact of magnetic fields on the evolution of LSS, the impact of BHs on LSS, the interplay between thermal and non-thermal phenomena in LSS.

Two approaches are here delineated to study these phenomena: i) a multi-frequency study of the various emission mechanism related to the previous phenomena; ii) a multi-purpouse technique, i.e. the Sunyaev-Zeldovich (SZ) effect in its most general derivation. We will discuss in the following some of the results obtainable along these two lines of investigation.

2 MULTI-FREQUENCY APPROACH

The phenomenology of galaxy clusters previously discussed indicates that a complex electron distribution is present in galaxy clusters' atmospheres: the superposition of electron populations of thermal, non-thermal, mild and fully relativistic nature provides a set of emission spectra spread over the whole electromagnetic (e.m.) spectrum, from radio to gamma-rays. A multi-frequency analysis is, therefore, optimally suited to disentangle the various components of the clusters' electron (and hadron) distribution and is able, in principle, to provide a detailed tomography of the atmospheres of galaxy clusters, and more generally of LSS. In the following, we will discuss how a multi-frequency analysis of e.m. signals visible from galaxy clusters is able to provide relevant information on various issues of the astro-particle physics of LSS.

2.1 The Nature of Dark Matter

The viable candidates proposed so far for a cosmologically relevant DM – neutralinos, sterile neutrinos, and more generally light DM particles – yield emission properties in DM halos that are markedly different and, therefore, allow a clear distinction of the relative DM nature.

Neutralinos which annihilate inside a DM halo produce quarks, leptons, vector bosons and Higgs bosons, depending on their mass and physical composition. Electrons are then produced from the decay of the final heavy fermions and bosons (see Fig. 1). The different composition of the $\chi\chi$ annihilation final

state will in general affect the form of the electron spectrum (see Fig. 2, see Colafrancesco & Mele 2001; Colafrancesco et al. 2006 for details).

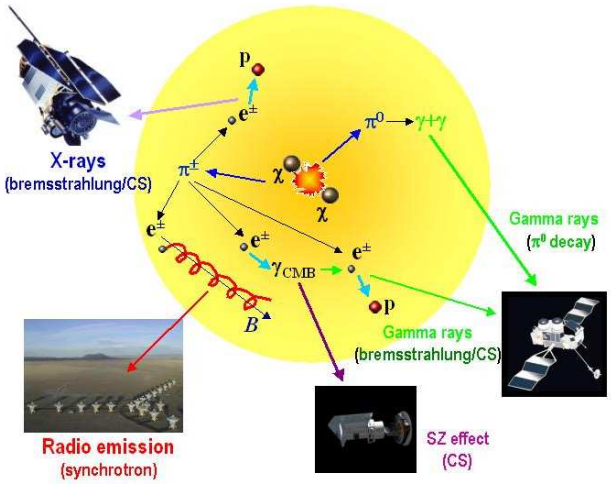

Fig. 1 A simple model which shows the basic astrophysical mechanisms underlying the search for the nature of DM particles (χ) through the emission features occurring in large-scale structures (e.g., galaxy clusters and galaxies). These mechanisms are, among others: γ-ray emission from $\pi^0 \rightarrow \gamma + \gamma$, relativistic bremsstrahlung of secondary $e^{\pm}$ and ICS of CMB photons by secondary $e^{\pm}$; X-ray/UV emission due to non-thermal bremsstrahlung and ICS of background photons by secondary $e^{\pm}$; synchrotron emission by secondary $e^{\pm}$ diffusing in the intra-cluster magnetic field; $\mathrm{SZ_{DM}}$ (ICS of CMB photons by secondary $e^{\pm}$) effect.

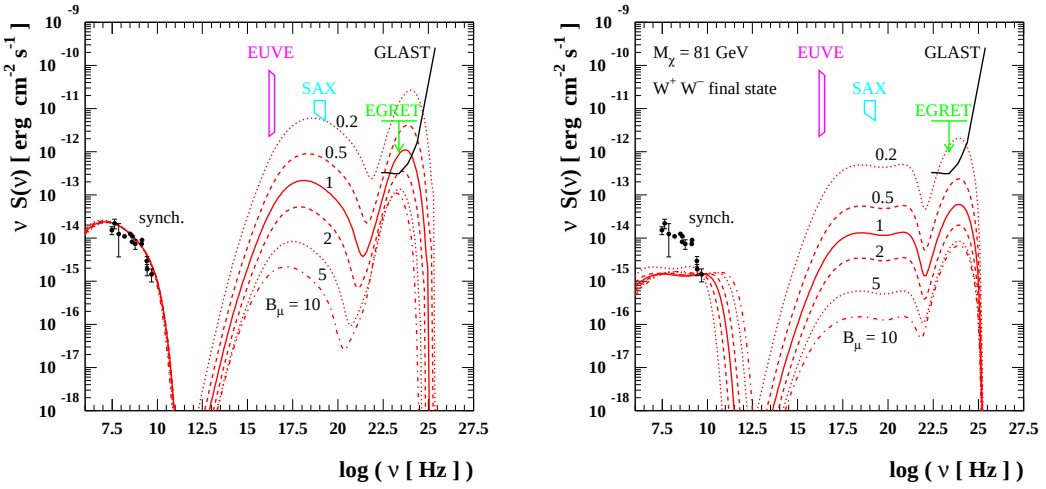

Fig. 2 Multi-frequency spectrum of Coma for the two DM models here considered (see Colafrancesco et al. 2006 for details): $M_\chi = 40$ GeV ($b\bar{b}$; left) and $M_\chi = 81$ GeV (W^+W^-; right). The halo profile is a NFW profile with $M_{\rm vir} = 9\,10^{14} M_\odot h^{-1}$ and $c_{\rm vir} = 10$, with subhalo setup as given in Colafrancesco et al. (2006). The scaling of the multi-frequency spectrum with the value for the mean magnetic field B_μ is shown for the two DM models.

The hadronic products of their annihilation ($\chi\chi \to X + \pi^0 \to \gamma\gamma$) provide a prompt gamma-ray emission with a characteristic spectrum peaked around the π^0 threshold energy and dying off at the neutralino mass energy scale.

The leptonic products of neutralino annihilation (secondary electrons produced through various prompt generation mechanisms and by the decay of charged pions $\pi^\pm \to \mu^\pm \nu_\mu(\bar{\nu}_\mu)$, with $\mu^\pm \to e^\pm + \bar{\nu}_\mu(\nu_\mu) + \nu_e(\bar{\nu}_e)$) are instead subject to spatial diffusion and energy losses. Both spatial diffusion and energy losses contribute to determine the evolution of the source spectrum into the equilibrium spectrum of these particles, *i.e.* the quantity which will be used to determine the multi-wavelength spectral energy distribution induced by $\chi\chi$ annihilation.

The time evolution of the secondary $e^\pm$ spectrum is described by the transport equation:

$$\frac{\partial n_e}{\partial t} = \nabla \left[D \nabla n_e \right] + \frac{\partial}{\partial E} \left[b_e n_e \right] + Q_e \ , \tag{1}$$

where $Q_e(E,r)$ is the $e^\pm$ source spectrum, $n_e(E,r)$ is the equilibrium spectrum and $b_e = b_{\rm ICS} + b_{\rm synch} + b_{\rm brem} + b_{\rm Coul}$, (given here in units of GeV s^{-1}) is the $e^\pm$ energy loss per unit time, with $b_{\rm ICS} \approx 2.5 \times 10^{-17} (E/{\rm GeV})^2$, $b_{\rm synch} \approx 2.54 \times 10^{-18} B_\mu^2 (E/{\rm GeV})^2$, $b_{\rm brem} \approx 1.51 \times 10^{-16} (n_{\rm th}/{\rm cm}^{-3}) \left(\log(\Gamma/n_{\rm th}) + 0.36 \right)$, $b_{\rm Coul} \approx 7 \times 10^{-16} (n_{\rm th}/{\rm cm}^{-3}) \left(1 + \log(\Gamma/n_{\rm th})/75 \right)$. Here $n_{\rm th}$ is the ambient gas density and $\Gamma \equiv E/m_e c^2$.

The population of these secondary $e^\pm$ can be described by a quasi-stationary ($\partial n_e/\partial t \approx 0$) transport equation, from which $n_e(E,r)$ reaches its equilibrium configuration mainly due to synchrotron and ICS losses at $E \gtrsim 150$ MeV and to Coulomb losses at smaller energies.

Diffusion affects in general the spatial and spectral shape of the signals coming from DM annihilation (see Colafrancesco 2005a); however, it can be neglected in galaxy clusters (Colafrancesco et al. 2006) while it is relevant on galactic and sub-galactic scales (Colafrancesco et al. 2007).

The secondary electrons eventually produce synchrotron radiation in the magnetized atmosphere of galaxy clusters, bremsstrahlung with ambient protons and ions and Inverse Compton Scattering (ICS) of CMB (and other background) photons and an SZ effect (see, e.g. Colafrancesco 2004b; see also Colafrancesco 2004a for a review). Hadrons and secondary electrons also produce heating of the ambient gas by Coulomb and hadronic collisions with the plasma particles. The astrophysical signals of DM annihilation can be visible, therefore, over the entire e.m. spectrum, from radio to γ-ray frequencies (see Fig. 2).

Gamma-ray emission is predominantly due to the hadronization of the decay products of $\chi\chi$ annihilation with a continuum γ-ray spectrum due to the decay $\pi^0 \to \gamma + \gamma$ (this is the most direct signal of $\chi\chi$ annihilation, see Colafrancesco & Mele 1998; Colafrancesco et al. 2006), even though the direct neutralino annihilation results in a line emission feature at an energy $\sim M_\chi$.

Gamma-ray emission is also expected from secondary $e^\pm$ produced by $\chi\chi$ annihilation. These secondary $e^\pm$ produce γ-rays through bremsstrahlung and ICS of CMB photons up to high energies (see Fig. 2). It could be revealed provided that i) sufficient spectral and spatial resolution can be achieved by the upcoming experiments and ii) a clear understanding of other competing emission mechanisms expected to work in cosmic structures (Colafrancesco 2004a for a review) will be obtained.

For the case of the Coma cluster, the gamma-ray flux produced by a soft $b\bar{b}$ neutralino model is dominated by the continuum $\pi^0 \to \gamma\gamma$ component and it is a factor ~ 5 lower than the EGRET upper limit of Coma at its peak frequency (see Fig. 2, left panel). Such gamma-ray flux could be, nonetheless, detectable by the GLAST–LAT detector at its peak energy. Harder W^+W^- neutralino models provide a quite different spectral energy distribution (see Fig. 2, right panel) and they can be therefore constrained by a full multi-frequency observational strategy. The rather low neutralino masses of these models make them rather difficult to be testable by Cherenkov gamma-ray detectors operating at higher threshold energies.

Secondary $e^\pm$ produced by $\chi\chi$ annihilation can produce synchrotron *radio emission* in the magnetized cluster atmosphere which could be observed as a diffuse radio emission centered on the DM halo. Observations of cluster radio-halos are, in principle, very effective in constraining the neutralino mass and composition (Colafrancesco & Mele 1998; Colafrancesco et al. 2006), under the hypothesis that DM annihilation provides a major contribution to the radio-halo flux.

Under this hypothesis, a pure energy requirement suggests that the neutralino mass is bound to be $M_\chi \geq 23.4\ \mathrm{GeV}(\nu/\mathrm{GHz})^{1/2}(B/\mu\mathrm{G})^{-1/2}$ in order to have secondary $e^\pm$ emitting at frequencies $\nu \geq 1$ GHz, as observed in cluster radio halos (see Feretti 2003 for a review).

The soft neutralino model ($b\bar{b}$ with $M_\chi = 40$ GeV), with the proper distribution of sub-halos, is able to reproduce both the overall radio-halo spectrum of Coma and the spatial distribution of its surface brightness (see Fig. 3), while the hard (W^+W^- with $M_\chi = 81$ GeV) model falls short of reproducing the shape of the Coma radio-halo spectrum.

Secondary $e^\pm$ *Compton up-scatter* CMB (and other background) photons that redistribute on a wide frequency range up to gamma-ray frequencies. The soft neutralino model with $M_\chi = 40$ GeV and $\langle\sigma v\rangle = 4.7 \times 10^{-25}\ \mathrm{cm}^3\ \mathrm{s}^{-1}$, with $B_\mu = 1.2$ (that reproduces the Coma radio-halo data) yields EUV and HXR fluxes which are more than one order of magnitude fainter than the Coma data (see Fig. 2).

Increasing the neutralino mass does not provide a decent fit of the radio-halo spectrum (see Fig. 2, right panel) and yields, in addition, extremely faint EUV, HXR and gamma-ray fluxes, which turn out to be undetectable even by GLAST and/or by the next coming high-energy experiments.

Increasing the annihilation cross-sections by a factor $\sim 10^2$ (i.e., up to values $\langle\sigma v\rangle \approx 7 \times 10^{-23}\ \mathrm{cm}^3\ \mathrm{s}^{-1}$) can fit the EUV and HXR data on Coma but the relative $\pi^0 \rightarrow \gamma\gamma$ gamma-ray flux at $E > 100$ MeV should exceed the EGRET limit on Coma.

Lowering the magnetic fields down to values $\sim 0.15\mu$G can fit both the HXR and the EUV fluxes of Coma but also in this case the $\pi^0 \rightarrow \gamma\gamma$ gamma-ray flux predicted by the same model at $E > 100$ MeV exceeds the EGRET limit on Coma, rendering untenable also this alternative. In conclusion, it is impossible to fit all the non-thermal data on Coma (see Fig. 2) for a consistent choice of the DM model and of the magnetic field (Colafrancesco et al. 2006).

We will discuss elsewhere further constraints on neutralino models that will be available from a multi-frequency analysis of the bullet cluster (1ES0657–556) where a spatial offset of the DM clumps w.r.t. the baryonic material is observed.

As for *sterile neutrinos*, their radiative decay $\nu_s \rightarrow \nu_i + \gamma$ (where ν_i indicate the standard low-mass neutrinos) produces a narrow line emission whose energy provides information on the sterile neutrino mass m_s. X-ray emission spectra from galaxy clusters are a powerful tool to set contraints on sterile neutrinos in the plane $m_s - \sin^2(2\theta)$. The available constraints on sterile neutrinos from X-ray spectra of clusters, combined with those obtained from the CXB, Lyα limits and gamma-ray line limits from the MW are shown in Figure 4. The constraints from Coma observations in the 20–80 keV band obtained here are shown by the cyan dashed area.

Models with lower mixing angles θ and neutrino masses m_s up to a few hundreds keV or $\gtrsim$ MeV are still available. In this case, next generation high-sensitivity hard X-ray detectors like SimbolX (Ferrando et al. 2005) or next coming soft gamma-ray experiments will be able to set relevant constraints to this DM model.

Other light DM candidates have been proposed so far (e.g., the MeV DM model) suggested to be responsible for the 511 keV annihilation line observed by INTEGRAL at the galactic center (Boehm et al. 2003) or Bose-Einstein condensates with $\gtrsim$ keV mass (Boyanovsky et al. 2007) and they could have visible e.m. features in galaxy clusters that we will address elsewhere.

2.2 The Origin of Cosmic Rays

Cosmic rays in clusters do certainly exist as a population of spatially diffused particles; in fact we record the signals of their interaction with the intra-cluster magnetic field through synchrotron radiation observed in many clusters. This radio emission can be divided into two categories that differ morphologically, in their degree of polarization and in their characteristic emission regions: the large-scale radio relics have a high degree of polarisation, are irregularly shaped and occur at peripheral cluster regions (see e.g. A3667, A3376, A2256), can be attributed to merging or accretion shock waves (see Pfrommer et al. 2007); the cluster radio halos seem to resemble the regular morphology of the X-ray emitting intra-cluster plasma (see e.g. Coma, 1E 0657–56), but its origin is not fully understood yet.

Hard X-ray excess observed in nearby clusters with radio halos (see Fusco-Femiano 2004 for a review) might confirm the existence of a diffuse population of CRs under the hypothesis that the HXR emission is

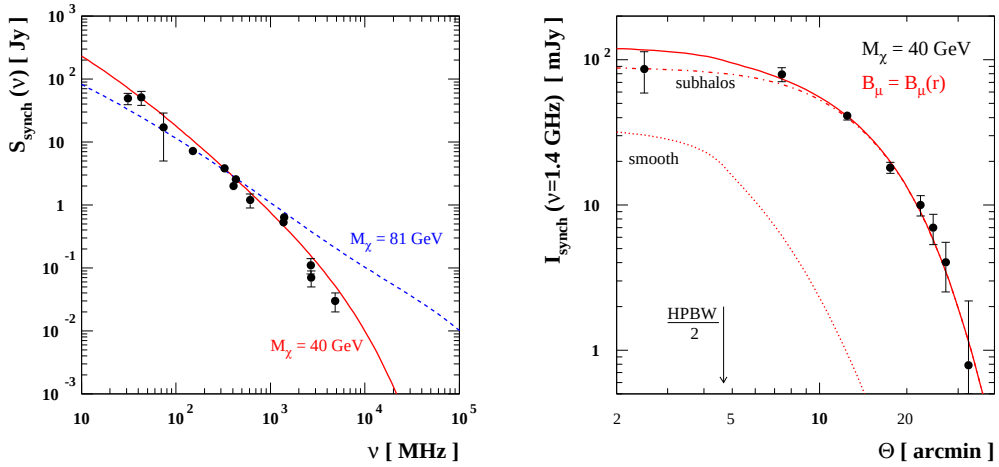

Fig. 3 **Left**. The radio flux density spectrum of Coma in two DM models: soft spectrum due to a $b\bar{b}$ annihilation final state (solid line) with $M_\chi = 40$ GeV) and hard spectrum due to a W^+W^- channel (dashed line) with $M_\chi = 81$ GeV). **Right**. Surface brightness distribution of Coma at $\nu = 1.4$ GHz, within a beam equal to $9'.35$ (HPBW), for the the lightest WIMP model. We consider a magnetic field $B(r) = B_0(1+(r/r_{c1})^2 \times [1+(r/r_{c2})^2]^{-\beta}$ with $B_0 = 0.55$ μG, $\beta = 2.7$, $r_{c1} = 3'$ and $r_{c2} = 17'.5$. The contributions from the smooth DM halo component only and from substructures only are also displayed (see Colafrancesco et al. 2006 for details).

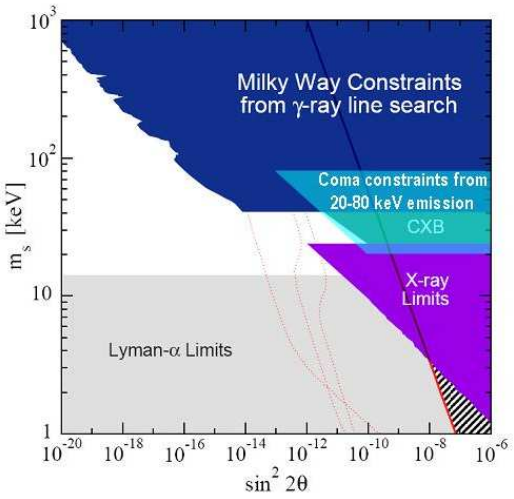

Fig. 4 The sterile neutrino mass m_s and mixing $\sin^2(2\theta)$ parameter space, with shaded regions excluded. The strongest direct bounds are shown, labeled as Milky Way (Yuksel et al. 2007), CXB (Boyarsky et al. 2006), and X-ray limits (summarized by Watson et al. 2006). The strongest indirect bounds (Seljak et al. 2006), Viel et al. (2006) are shown by the grey horizontal band. The excluded Dodelson-Widrow model (Dodelson & Widrow 1994) is shown by the solid line; rightward, the DM density is too high (stripes). The dotted lines indicate example models (see Abazajian & Fuller 2002), now truncated by the available constraints. The cyan shaded area indicates our constraints from the HXR (soft gamma-ray) limit on Coma (this paper). Figure adapted from Yuksel et al. (2007).

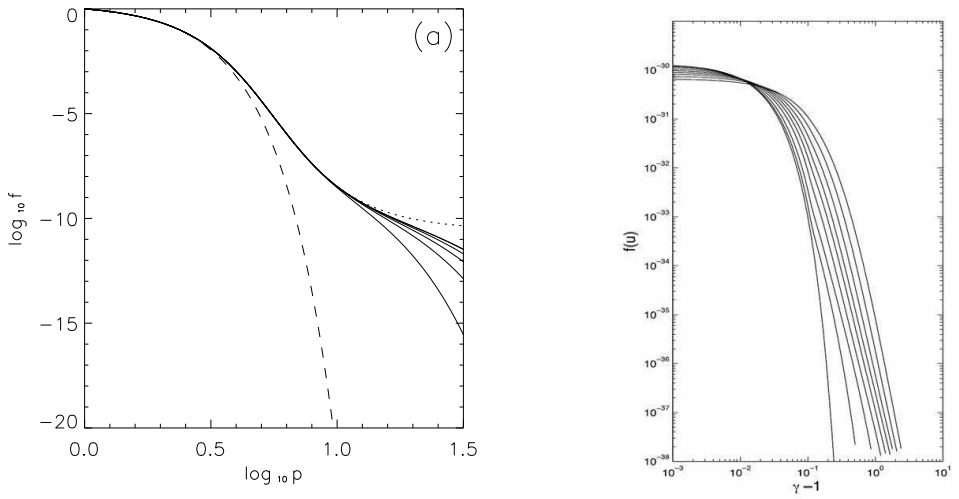

Fig. 5 Left.The time evolution of the distribution function of turbulent accelerated electrons in the cluster atmosphere up to $t = 1.85$ Gyr after acceleration is switched on. The initial distribution (dashed curve) is Maxwellian. Figure from Dogiel et al. (2007). **Right**. Evolution of the electron distribution from a Maxwellian equilibrium distribution at $T = 7.5$ keV under the action of turbulent diffusion: moving progressively rightward the curves are evaluated at $t = 0, 4.5, 18, 36, 54, 72, 90, 108$, and 126 Myr. Figure from Wolfe & Melia (2006).

predominantly due to Inverse Compton Scattering (ICS) of CMB photons off the low-energy part of the CR spectrum.

A basic problem stands out with the origin of the CRs supposedly producing the radio halo feature. Two general mechanisms have been explored so far: i) direct or stochastic acceleration and/or re-acceleration caused by merging shocks and turbulence; ii) in-situ, (quasi-) stationary production mechanisms like pp collisions.

It has been recently shown that shock acceleration in cluster atmosphere is not efficient on time scales $\lesssim 2 \times 10^7$ yr because the energy gained by the particles is actually redistributed to the whole IC plasma on a timescale much shorter than that of the acceleration process itself (see Fig. 5 and Wolfe & Melia 2006). It has also been shown that turbulent acceleration of particles out of the IC gas thermal pool can produce a quasi-stationary, supra-thermal region where particles actually may gain energy but they don't have sufficient time to produce a power-law spectrum extending to relativistic energies, like that required to explain radio-halo emission (see Fig. 5 and Dogiel et al. 2007).

Recent attempts to explain the non-thermal emission in galaxy clusters have been proposed as a result of the re-acceleration of electrons by turbulence induced by cluster mergers (Cassano & Brunetti 2004; Cassano et al. 2007; Brunetti & Lazarian 2007). Such models assume the presence of a population of relativistic electrons in the ICM which are continuously injected by AGNs, Galactic Winds, and/or merger shocks. The electron-acceleration efficiency is calculated considering all the merger events which contribute to the injection of turbulence in the considered cluster. This condition has to contend, however, with the efficiency of thermalization of such relativistic particles which seems quite high in the ICM (see Wolfe & Melia 2006).

In-situ production of secondary electrons by pp collisions rely on the possibility to accumulate and store CR hadrons in clusters for long time scales (see Colafrancesco & Blasi 1998) and can produce a radio halo spectrum whose shape is strictly related to that of the parent CR protons and yet in agreement with the radio halo spectra, when no high or low radio frequency curvature is very prominent (Marchegiani et al. 2007). In addition, this model can easily be tested against the observations of gamma-ray emission from the same radio-halo clusters with the next coming GLAST experiment (see Fig. 6).

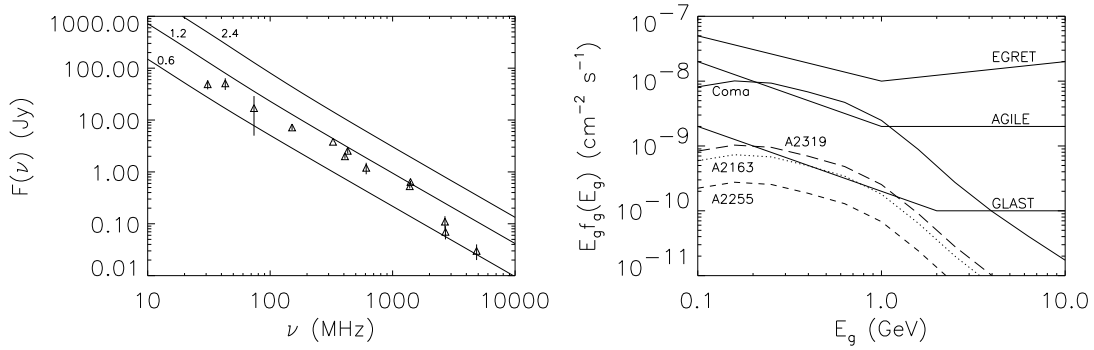

Fig. 6 **Left**. The radio flux density spectrum of Coma in produced by secondary electrons in an in-situ pp collision model. The initial CR proton spectrum slope s is shown. **Right**. The gamma-ray spectra of several radio-halo clusters whose spectrum can be recovered in a pp collision model, are compared with the sensitivity of EGRET, AGILE and GLAST-LAT. Figures from Marchegiani et al. (2007).

The alternative model in which highly relativistic secondary electrons (with $E_e \sim 10^{15} - 10^{16}$ eV) are produced by the interaction of UHECRs with CMB photons and fitted to recover the HXR emission spectrum of clusters by synchrotron radiation, predicts a ICS emission which extends up into the TeV range where Cherenkov telescopes can test this hypothesis, but hardly fails to reproduce the radio-halo emission (Inoue et al. 2005). This model largely relies on the possibility to have very strong sources of CR hadrons (likely replicas of M87 and CenA) located in the cluster environment, an assumption that could eventually tested with the next high-sensitivity gamma-ray telescopes operating in the GeV – TeV range (like CTA).

In conclusion, it is clear that a full multi-frequency study of CR interactions in clusters' atmospheres will be able to disentangle the various mechanisms so far proposed for their origin.

2.3 The Impact of Black Holes in Galaxy Clusters.

CRs can also be injected in the cluster atmosphere by the jets of AGNs which are settling in the clusters' potential wells. Supermassive BHs in the cluster's core generate, in fact, jets and lobes filled with non-thermal, relativistic particles which are both directly injected into the ambient medium and/or confined in buoyant bubbles. The relativistic particles injected in this way can both diffuse in the ambient medium and accumulate into the cluster environment, eventually reaching a quasi-stationary equilibrium condition with the cluster's material, or remain locked in non-thermal bubbles until they are released, at a subsequent stage, into the ambient medium.

The complex admixture of a thermal atmosphere in which AGNs and non-thermal bubbles are embedded can be optimally studied using multi-frequency observations of clusters, from radio to gamma-rays. In fact, while the cluster's thermal component dominates the cluster emission at X-ray ($\sim 0.1 - 10$ keV) energies, the hard X-ray band at $E \gtrsim 20$ keV can reveal the presence of the non-thermal emission emerging from both the central AGN and from the associated relativistic plasma bubbles (if their electron spectra are rather flat). Therefore, the next generation HXR spectro-imaging observations of clusters obtainable with SimbolX in the 10–80 keV band, will be able to separate spatially the different spectral components associated to the thermal plasma and to the non-thermal cavities. If the non-thermal plasma inside cavities reaches relativistic energies, the coming GLAST-LAT experiment could detect in several objects the additional gamma-ray emission produced in the non-thermal bubbles and disentangle them from the overall cluster gamma-ray emission using the multi-frequency correlation with the HXR images and the radio emission generated by the same bubbles.

In addition to the previous phenomena, the non-thermal activity triggered by the BHs at the cluster centers might produce a feedback onto the IC gas that could help in quenching its radiative cooling. It is becoming clear, in this context, that the non-thermal heating must be distributed in a way to adapt itself to

the IC gas cooling, i.e. with a similar pressure distribution $P_{\rm non-th} \sim P_{\rm th}$, as it is the case shown by the Perseus cluster (see Sanders & Fabian 2007).

Under the reasonable assumption that CRs are produced in cluster cores and diffuse away to adapt themselves to a radial distribution similar to that of the IC gas, $n_{\rm CR} \propto [n_e(r)]^{\alpha}$ (see Colafrancesco & Marchegiani 2007), they provide a quasi-stationary equilibrium condition

$$3\,k\,n_{\rm e}(r)\,\frac{dT(r,t)}{dt} = \left.\frac{d\epsilon}{dt}\right|_{\rm CR} - \left.\frac{d\epsilon}{dt}\right|_{\rm X}\,, \qquad (2)$$

that is able to reproduce the temperature and entropy structure of cluster cores (see Colafrancesco & Marchegiani 2007; Colafrancesco, Dar & DeRujula 2004). This warming-ray (WR) model predicts specific correlations between the thermal and non-thermal properties of galaxy clusters. The temperature distribution of the IC gas in both cool-core and non cool-core clusters is successfully predicted from the observed IC plasma density distribution. Using this constraint, the WR model is also able to reproduce the thermal and non-thermal pressure distribution in clusters, as well as their radial entropy distribution, as shown by the analysis of three clusters studied in details: Perseus, A2199 and Hydra. The WR model predicts other observable features of galaxy clusters: a correlation of the pressure ratio (WRs to thermal IC gas) with the inner cluster temperature $(P_{\rm WR}/P_{\rm th}) \sim (kT_{\rm inner})^{-2/3}$, a correlation of the gamma-ray luminosity with the inner cluster temperature (see Fig. 7), a substantial number of cool-core clusters observable with GLAST-LAT experiment, a surface brightness of radio halos in cool-core clusters that recovers the observed one, a hard X-ray ICS emission from cool-core clusters that is systematically lower than the observed limits and yet observable with the next generation high-sensitivity and spatial resolution HXR experiments like SimbolX. The specific theoretical properties and the multi-frequency distribution of the e.m. signals predicted in the WR model make it possible to prove or disprove this model as an explanation of the cooling-flow problems on the basis of multi-frequency observations of galaxy clusters.

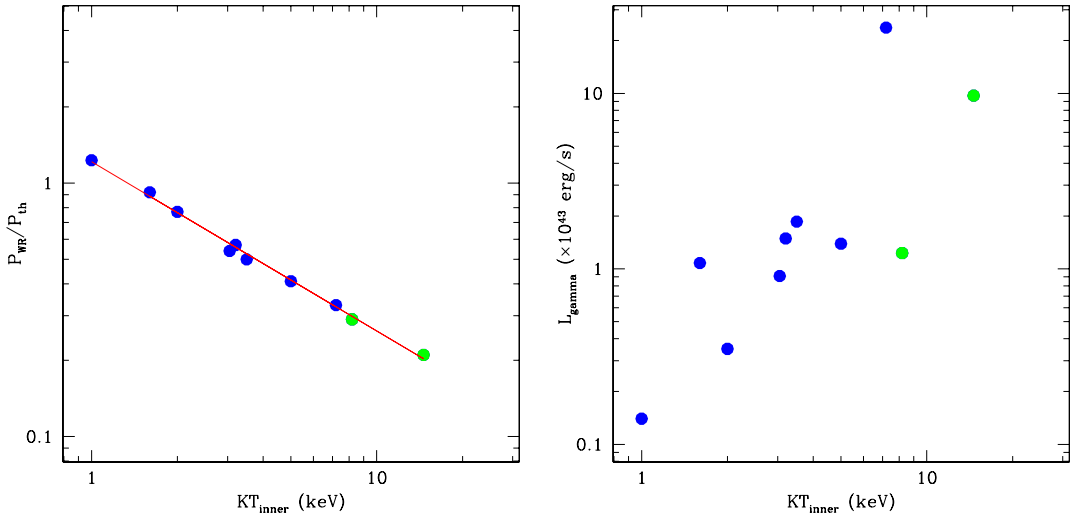

Fig. 7 **Left**. The correlation of the central pressure ratio $P_{\rm WR}/P_{\rm th}$ with the inner temperature of the cool core $T_{\rm inner}$ in keV is given for ten best studied clusters (see Colafrancesco & Marchegiani 2007). The fit $P_{\rm WR}/P_{\rm th} \propto (kT_{\rm inner})^{-2/3}$ is shown as a solid line. Blue dots refer to cool-core clusters and green dots to non cool-core clusters. **Right**. The correlation of the gamma-ray luminosity L_γ with the inner temperature of the cool core $T_{\rm inner}$. Blue dots refer to cool-core clusters and green dots to non cool-core clusters.

2.4 Magnetic Fields in Cluster Atmospheres

In order to confine CRs in clusters' atmospheres, a magnetic field B is required. Such a B-field has also a relevant impact on the main structural properties of clusters and groups of galaxies (Colafrancesco & Giordano 2006, 2007). It affects the radial density and entropy profiles, the entropy – temperature relation and the X-ray luminosity – temperature relation for groups and clusters of galaxies. A description of the intra-cluster gas based on the Magnetic Virial Theorem

$$2U + U_B + W = 0 \tag{3}$$

(here U is the kinetic energy, W is the potential energy and U_B is the magnetic energy of the system), and on the Hydrostatic Equilibrium condition (Colafrancesco & Giordano 2007)

$$\frac{dP_g}{dr} + \frac{dP_B}{dr} = -\frac{GM(\leq r)}{r^2}\rho_g \ , \tag{4}$$

where $\rho_g \equiv \rho_g(r, B)$ is the density of the thermal IC gas and $P_g(r, B)$ is its pressure, with both quantities depending in general on the magnetic field $B(r) = B_*(\rho_g(r))^\alpha$ (with $\alpha \approx 0.9$, as the one indicated by observations and numerical simulation), is able to provide, at once, a possible explanation of many problematic aspects of the cluster structure: i) the flattening of the entropy profile in the cluster center (together with the possible entropy inversion near their centers); ii) the flatness of the $S - T$ relation (together with the entropy inversion at the scale of the galaxy groups); iii) the increasing steepening of the $L_{\rm X} - T$ relation from the cluster scale towards the group scales (Colafrancesco & Giordano 2007). The available entropy and X-ray luminosity data indicate that a scaling of the magnetic field $B_* \sim T^{0.5\pm0.1}$ is required to reproduce, at the same time, both the $S - T$ and the $L_{\rm X} - T$ relations. The values of the central B-field inferred by the previous scaling seem to be consistent with those inferred in clusters' cores by Faraday Rotation measures (see Colafrancesco & Giordano 2007). Thus, a consistent description of the magnetized ICM can provide a simple explanation of several (or of all) of these still open problems, and thus weakens the need for the inclusion of other non-gravitational effects which have been proposed so far for the explanation of some of these features. This analysis can be regarded as a starting point for a more refined exploration of the physics of the magnetized ICM, and it provides testable predictions that can be proven or disproven with the next coming sensitive observations of groups and clusters in the X-ray band and in the radio frequency band, where the B-field contributes crucially to the synchrotron emission.

3 A SINGLE-TECHNIQUE APPROACH: THE SZ EFFECT

So far, we have shown that a multi-frequency analysis is able to study and disentangle the various particle families and fields constituting the atmospheres of galaxy clusters. Such a strategy requires a combined synergy from different experiments and different theoretical approaches: in this sense it is a demanding task but it will return, nonetheless, unvaluable information on many themes of the present-day Astro Particle Physics research, from the nature of Dark Matter to the origin of CRs, from the impact and evolution of large-scale B-field to the physical feedback of BHs in cosmic structures.

It is interesting to note that all of these themes can be also played by using a single instrument: the Sunyaev–Zel'dovich effect (1980) in its most general derivation (see, e.g. Colafrancesco 2007a for a review). According to the generalized expression for the SZE which is valid in the Thomson limit for a generic electron population, in the full relativistic treatment and includes also the effects of multiple scatterings and the combination with other electron populations (see Colafrancesco et al. 2003), the spectral distortion observable in the direction of a galaxy cluster can be written as

$$\Delta I(x) = 2\frac{(k_{\rm B}T_{\rm CMB})^3}{(hc)^2} y\, g(x) \ , \tag{5}$$

where the Comptonization parameter y is given by

$$y = \frac{\sigma_T}{m_{\rm e}c^2}\int P_{\rm e} d\ell \ , \tag{6}$$

in terms of the pressure $P_{\rm e}$ contributed by the specific electron distribution within the cluster. The function $g(x)$ for the considered electron population can be written as

$$g(x) = \frac{m_{\rm e}c^2}{\langle k_{\rm B}T_{\rm e}\rangle}\left\{\frac{1}{\tau}\left[\int_{-\infty}^{+\infty} i_0(xe^{-s})P(s)ds - i_0(x)\right]\right\}, \quad (7)$$

in terms of the photon redistribution function $P(s)$, of the undistorted CMB spectrum $i_0(x) = \frac{2(k_{\rm B}T_{\rm CMB})^3}{(hc)^2}\times \frac{x^3}{(e^x-1)}$, and of the average energy density

$$\langle\varepsilon\rangle \equiv \frac{\sigma_{\rm T}}{\tau}\int P_e d\ell = \int_0^\infty dp f_{\rm e}(p)\frac{1}{3}pv(p)m_{\rm e}c. \quad (8)$$

The photon redistribution function $P(s) = \int dp f_{\rm e}(p)P_{\rm s}(s;p)$ with $s = \ln(\nu'/\nu)$, in terms of the CMB photon frequency increase factor ν'/ν, contains the crucial dependence on the electron momentum distribution $f_{\rm e}(p)$, where p is normalized to $m_e c$. Here $P_{\rm s}(s;p)$ is the mono-energetic frequency redistribution function.

The spectral function of the SZE evaluated for various electron spectra is shown in Figure 8. It is clear that the different nature of the electron distribution reflects directly in the different spectral shape of the relative SZE. Thus, the SZE is a powerful probe of the energy spectrum of the various electronic populations residing in the atmospheres of cosmic structures.

We will describe in the following the relevance of the SZE to the study of several different aspects of the astro-particle physics of galaxy clusters previously addressed using the multi-frequency strategy.

Testing the acceleration history of cosmic rays

Whatever the mechanism that accelerate particles is, thus producing non-thermal or quasi-thermal spectral tails, it should be extremely efficient to beat the competing thermalization process for such high-energy particles (see, Wolfe & Melia 2006; Dogiel et al. 2007). As a result, the viable models produce rather different non-thermal or quasi-thermal electron spectra whose nature can be constrained by studying the associated SZE (see Fig. 9). If the acceleration is so efficient to produce a high-E power-law tail, the SZE attributed to the relativistic electrons that produce the cluster radio-halo spectra is expected to be completely negative at all the frequencies relevant for the SZ experiments ($\nu \sim 20 - 350\,$GHz) and with an amplitude of a few percent of the thermal SZE in the cluster which renders its detection quite challenging. On the other hand, the SZE effect produced by quasi-thermal electrons stochastically accelerated in the cluster environment is expected to produce a detectable CMB temperature decrement $\Delta T \sim 40 - 50\ \mu$K at low frequencies (see Fig. 9) that could prove or set relevant constraints to this scenario as well as to the efficiency of thermalisation and acceleration processes. In the case of inefficient shock acceleration, an increase of the average plasma temperature is provided by the thermalization of high-energy particle which, in turn, yields a SZE with thermal features (Fig. 9).

Testing the content and the energetics of cluster cavities

While the properties of clusters' cavities and of the relativistic plasma they contain is usually studied by combining high-resolution X-ray and radio maps, we have proposed (Colafrancesco 2005b), as an alternative strategy, to study the consequences of the Compton scattering between the high-energy electrons filling the cavities and the CMB photon field (i.e. the SZE) whose amplitude, spectral and spatial features depend on the overall pressure and energetics of the relativistic plasma in the cavities (see Fig. 10 and Colafrancesco 2005b for the specific case of the cluster MS0735+7421).

At frequencies $x \sim 2.5$ there is the maximum amplitude of the non-thermal SZE from the cavity (for a given electron spectrum and pressure). This produces a bump in the spatial distribution of the overall SZE at the cavity location with the addition of a negative SZE signal to the thermal SZE of the cluster. At $x > x_{0,\rm th}(P_{\rm th})$ – where $x_{0,\rm th}$ is the crossover frequency at which the thermal SZE is null – we have the opposite effect but with smaller amplitudes: a depression in the SZE at the cavity location caused by the addition of a negative SZE signal to the positive thermal SZE. We emphasize that SZ observations at the frequency $x = x_{0,\rm th}(P_{\rm th})$ (which is ≈ 3.87 for a $k_BT = 5$ keV cluster) provide a unique way to probe the overall energetics, the pressure and the spatial extent of the non-thermal plasma contained in

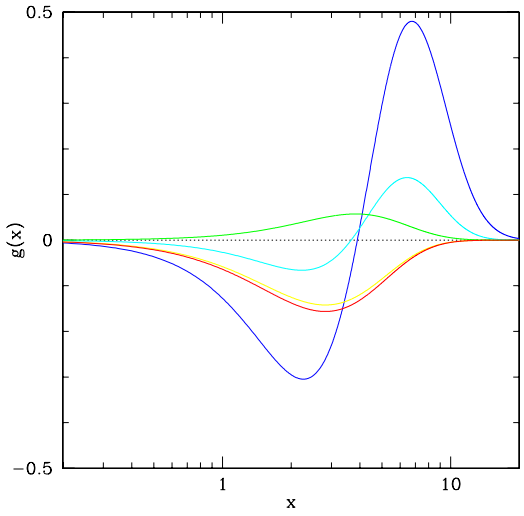

Fig. 8 The function $g(x)$ is shown as a function of the adimensional frequency x for different electronic populations residing in the cluster atmosphere: thermal with $k_B T_e = 8.2$ keV (blue); warm with $k_B T_e = 1$ keV (cyan); secondary electrons from DM annihilation with $M_\chi = 20$ GeV (red); relativistic electrons which fit the Coma radio halo integrated spectrum (yellow). Also the kinematic SZE with a negative peculiar velocity (green) is shown for comparison. The amplitudes of the various curves have been artificially re-normalized to highlight their frequency dependence.

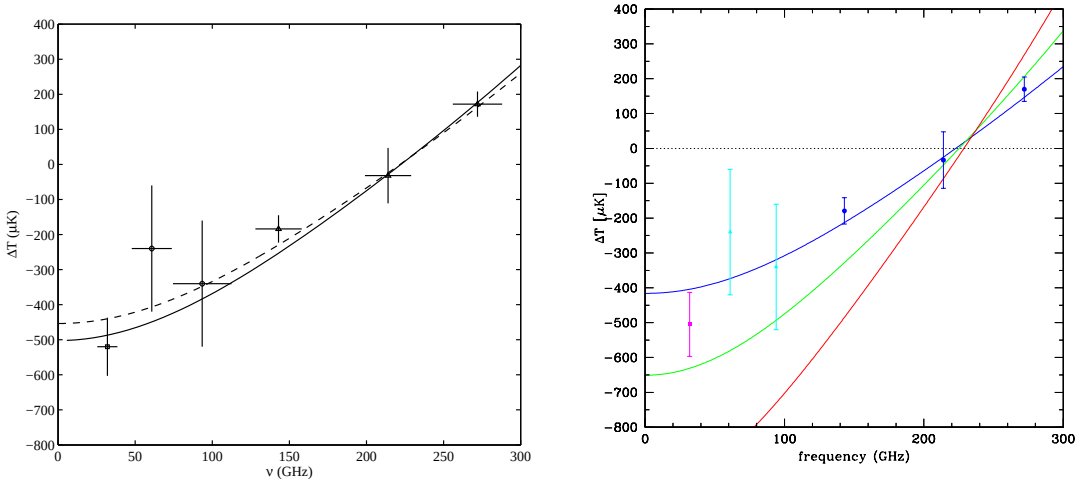

Fig. 9 **Left:** The SZE from the quasi-thermal particle distribution that fits the HXR emission of Coma in a stochastic acceleration scenario (solid curve, Dogiel et al. 2007). The dashed curve shows the thermal SZE expected from Coma. **Right:** The SZE from inefficient shock acceleration (see Wolfe & Melia 2006) is expected to produce a pure thermal SZE at temperatures larger than the initial ICM temperature of Coma: the different curves refer to values $kT = 8$ (blue), 13 (gren) and 20 (red) keV.

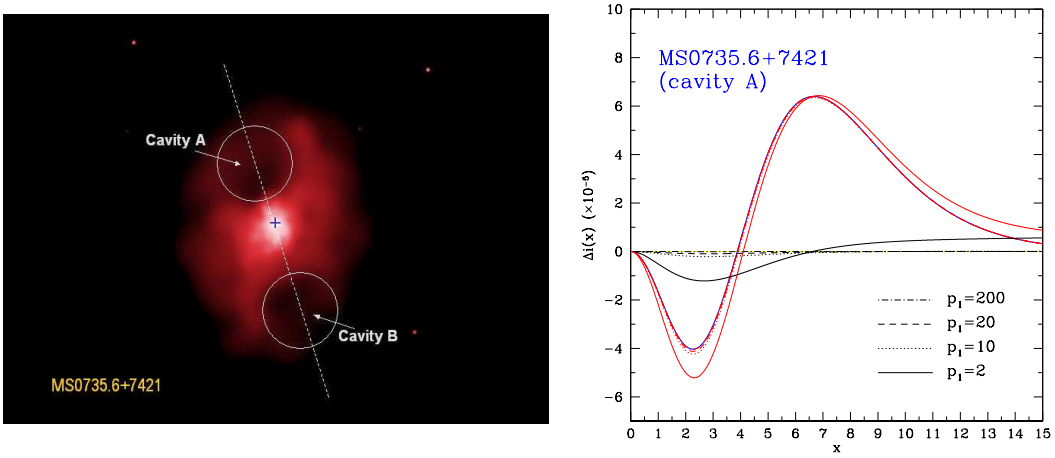

Fig. 10 **Left:** The geometry of the cavities in the cluster MS0735.6+7421 is shown. The two cavities have a radius ≈ 100 kpc and are located at a distance of ≈ 125 kpc and ≈ 170 kpc from the central radio galaxy (whose position is indicated by a cross) along the axis represented in the picture. **Right:** The spectrum of the overall SZE from the cluster MS0735.6+7421 has been computed at a projected radius of ≈ 125 kpc from the cluster center where the los passes through the center of cavity A. We show the thermal SZE (blue), the non-thermal SZE from the cavity (black) and the total SZE (red). The plotted curves are for different values of the lowest electron momentum: $p_1 = 200$ (dot-dashes), $p_1 = 20$ (dashes), $p_1 = 10$ (dots) and $p_1 = 2$ (solid). The non-thermal SZE is normalized to the cavity pressure $P = 6 \times 10^{-11}$ erg cm^{-3}.

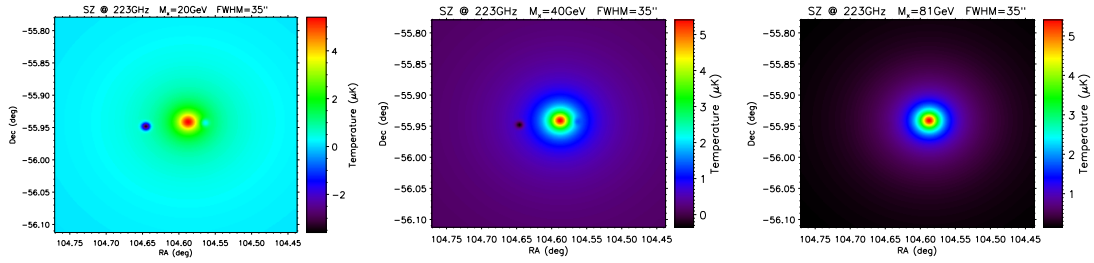

Fig. 11 Simulated SZ maps of the cluster 1ES0657–556 as observable with the SPT at $\nu = 223$ GHz for three different χ masses: $M_\chi = 20$ GeV (left panel), 40 GeV (mid panel) and 81 GeV (right panel) (see Colafrancesco et al. 2007 for details).

giant cavities, an observation which is rich in information and complementary to those obtained by X-ray and radio observations of cluster cavities. At this frequency, in fact, the overall SZE from the cluster reveals only the Compton scattering of the electrons residing in the cavities without the presence of the intense thermal SZE from the cluster's thermal atmosphere observable at lower and higher frequencies. Hence, the SZE from a cluster containing cavities (like the case of MS0735.6+7421) shows up uncontaminated at frequencies ~ 220 GHz: it is less extended than the overall cluster SZE because it is only emerging from the cavity regions and it is also well separable because the cavities are well defined in both X-rays and SZ images. We also emphasize that the observation of the zero and of the spectrum of the non-thermal SZE in the cavities provide a definite way to determine uniquely the total pressure and hence the nature of the electron population within the cavity, an evidence which adds crucial, complementary information to the X-ray and radio analysis. Even though the determination of the crossover frequency $x_0(P_e)$ can be

biased by possible sources of additional SZE (e.g., the kinematic SZE or the SZE coming from additional electron components), a full spectroscopic study of the SZE around the zero of the thermal SZE will provide unbiased information on the various electron populations in clusters (Colafrancesco, Prokhorov & Dogiel 2007). These studies will be also relevant to determine the impact of specific events like cavities on the use of SZE and X-ray clusters as probes for cosmology and for the evolution of large scale structure of the universe.

SZE and the nature of Dark Matter

Dark Matter annihilations in the halo of galaxies and galaxy clusters have relevant astrophysical implications, even for SZE observations. Colafrancesco (2004b) proposed to explore the consequences of the Compton scattering between the secondary electrons produced from the WIMP annihilation in massive DM halos (like galaxy clusters and dwarf galaxies) and the CMB photon field, i.e. the DM-induced SZE which has specific spectral and spatial features. This is an inevitable consequence of the presence and of the nature of DM in large-scale structures.

The analysis of the DM induced SZE in galaxy clusters provides a probe for the presence and for the nature of DM in cosmic structures which is complementary to those obtainable through a multifrequency analysis (see Sect. 2). The available SZ observations on the Coma cluster (see Colafrancesco 2004b) can already set a lower limit to the neutralino mass of $M_\chi \gtrsim 17 - 20$ GeV ($M_\chi \gtrsim 13$ GeV at 90% c.l. with the adopted value of $\langle\sigma v\rangle_0 = 3 \times 10^{-27}$ cm^{-3} s$^{-1}/\Omega_\chi h^2$ with $\Omega_\chi h^2 = 0.116$). The SZ$_{\rm DM}$ signal does not strongly depend on the assumed DM density profile at intermediate angular distances from the cluster center and on the DM clumpiness since $y_{\rm DM} = (\sigma T/m_e c^2)\int d\ell P_{\rm e,DM}$ is the integral of the secondary electron pressure, $P_{\rm e,DM}$, along the line of sight.

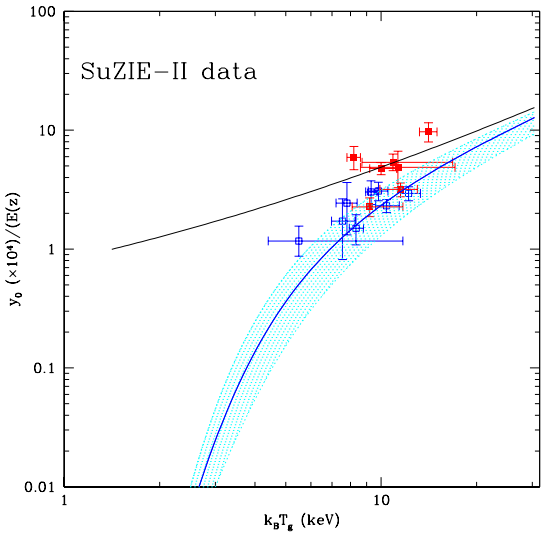

Fig. 12 The $y_{\rm th}(0) - T_g$ relation for $B_* = 0$ (black curve) is compared with that calculated assuming the scaling $B_* \propto T^\eta$ (cyan shaded area) which best fits the $S - T$ and $L_{\rm X} - T$ relations for clusters (Colafrancesco & Giordano 2007). Data are from the SuZIE II experiment (Benson et al. 2004): filled squares refer to clusters with cool cores while open squares refer to clusters without cool cores. Figure from Colafrancesco (2007b).

The presence of a substantial SZ$_{\rm DM}$ effect is likely to dominate the overall SZ signal at frequencies $x \gtrsim 3.8 - 4.5$ providing a negative total SZE (see Fig. 8). Even though in such frequency range there are other possible contributions to the SZE, like the kinematic effect and the non-thermal SZE which could provide additional biases (see, e.g., Colafrancesco et al. 2003). An appropriate spectroscopic analysis of the

overall SZE is required, in principle, to separate the various SZ contributions and to provide an estimate of the DM induced SZE. A particularly good case in which the $\mathrm{SZ_{DM}}$ could be revealed is that of the cluster 1E0657–556 where the $\mathrm{SZ_{DM}}$ signal is peaked on the DM clumps, and is well separated (by several arcmin) from the thermal SZE concentrated on the X-ray emitting IC gas location and from the non-thermal SZE associated with the shock. In this case, the $\mathrm{SZ_{DM}}$ signal is the only one remaining at frequencies $x = x_{\mathrm{o,th}}$ at the DM clump locations (see Fig. 11, see Colafrancesco et al. 2007). Future SZ experiment with $\sim \mu$K sensitivity (and $\lesssim$ arcmin angular resolution) could be able to detect direct signals from DM annihilation in the most favourable supersymmetric scenarios.

SZE and magnetic fields. There are also non-standard aspects of the widely-used thermal SZE that need to be carefully and specifically addressed. In particular, the presence of an intra-cluster magnetic field can produce relevant changes to the thermal SZE in galaxy clusters (Colafrancesco 2007b).

The presence of a wide-scale magnetic field implies modification on the thermal and density structure of the IC gas by acting on both the magnetic virial theorem and the hydrostatic equilibrium condition (Colafrancesco & Giordano 2006, 2007). As a consequence, the cluster thermal SZE is influenced by the presence of an intracluster magnetic field, as shown in Figure 12. For idealized isothermal clusters, the magnetic SZE is reduced w.r.t. the unmagnetized case by two separate effects: i) the decrease in the cluster temperature as derived by the MVT (see Eq. (3)) for increasing values of B; and ii) the decrease of the central IC gas density profile according to the HE condition (see Eq. (4)) for increasing values of B. The variations of the thermal SZE for magnetized clusters is larger for lower-mass systems because in these structures the pressure provided by the magnetic field is of larger relative importance w.r.t. to the thermal pressure of the IC gas settling in the potential wells provided by DM. This allows to reproduce the steepening of the $y_0 - T$ relation shown by the most recent data (see Fig. 12). The increasing observational evidence, the refinements of numerical simulations and the theoretical expectations for the presence of magnetic fields in galaxy clusters render a revision of the standard description of the thermal SZE necessary to describe both single SZ observations and SZ scaling-law analyses in a self-consistent astrophysical and cosmological framework (see discussion in Colafrancesco 2007a).

4 EPILOGUE

Astro Particle Physics poses many fundamental questions on the structure and evolution of LSS that begin to find a theoretical and experimental test bed in galaxy clusters, the largest laboratories for APP in the universe. Two basic approaches can fulfill this task: i) a multi-frequency analysis, that requires a combined, challenging synergy from different experiments and different theoretical approaches; ii) a multi-purpouse tool, the SZ effect, that is able to probe the physical impact of each particle family and radiation fields through a single experimental, but sensitivity-challenging technique. The task is anyway demanding but it will return, when achieved, invaluable information on many themes of the present-day Astro Particle Physics research, from the nature of Dark Matter to the origin of CRs, from the impact and evolution of large-scale B-field to the physical feedback of BHs in cosmic structures. This information is not only precious for its astrophysical impact but is also crucial for the possible cosmological use of galaxy clusters as probes of the structure of the universe.

Acknowledgements S.C. thanks P. Giommi, A. Fabian, S. Schindler, J. Beall, G. Auriemma, A. DeRujula, A. Dar for interesting and stimulating discussions, and Amiya Dar for her artistic touch.

References

Abazajian F., 2002, Phys. Rev. D., 66, 023526
Bagchi J. et al., 2002, arXiv:astro-ph/0204389
Benson B. A., 2004, ApJ, 617, 829
Birzan L. et al., 2004, ApJ, 607, 800
Boehm C. et al., 2004, Phys.Rev.Lett. 92 101301
Boyarsky A. et al., 2006, MNRAS, 370, 213
Boyanovsky D., de Vega H. J., Sanchez N., 2007, (arXiv:0710.5180)

Bregman J., 2003, in: Reiprich T. H., Kempner J. C., Soker N. eds., Proceedings of The Riddle of Cooling Flows in Galaxies and Clusters of Galaxies
Brunetti G., Lazarian A., 2007, arXiv:astro-ph/0703591
Caffi S., Gastaldello F., Molendi S., 2004, 35th COSPAR Scientific Assembly, p.2824
Carilli C. L., Taylor G. B., 2002, ARAA, 40, 319
Cassano R., Brunetti G., 2004, JKA, 37, 5, 583 (arXiv:astro-ph/0412325)
Cassano R. et al., 2007, arXiv:0712.3516
Colafrancesco S., 2004a, in: A. Blanchard, M. Signore, eds., Frontiers of cosmology, NATO science series II: Mathematics, physics and chemistry, Vol. 187, Dordrecht: Springer, 2005, p.85
Colafrancesco S., 2004b, A&A, 422, L23
Colafrancesco S., 2005a, in: Jerjen H., Binggeli B. eds., Near-fields cosmology with dwarf elliptical galaxies, Proceedings of the IAU 198, Cambridge: Cambridge University Press, p.229
Colafrancesco S., 2005b, A&A, 435, L9
Colafrancesco S., 2007, New Astron.Rev., 51, 394
Colafrancesco S., 2007, A&A, submitted
Colafrancesco S., Blasi P., 1998, APPhys., 9, 128
Colafrancesco S., Mele B., 2001, ApJ, 562, 24
Colafrancesco S., Marchegiani P., Palladino E., 2003, A&A, 397, 27
Colafrancesco S., Dar A., DeRujula A., 2004, A&A, 413, 441
Colafrancesco S., Profumo S., Ullio P., 2006, A&A, 455, 21
Colafrancesco S., Giordano F., 2006, A&A, 454, L131
Colafrancesco S., Profumo S., Ullio P., 2007, PhRvD, 75, 3513
Colafrancesco S. et al., 2007, A&A, 467, L1
Colafrancesco S., Giordano F., 2007, A&A, 466, 421
Colafrancesco S., Marchegiani P., 2007, A&A, submitted
Colafrancesco S., Prokhorov D., Dogiel V., 2007, A&A, submitted
Dodelson S., Widrow A., 1994, Phys. Rev. Lett. 72, 17
Dogiel V. et al., 2007, A&A, 461, 433
Dolag K. et al., 2004, arXiv:astro-ph/0410419
Donahue M. et al., 2006, ApJ, 643, 730
Eilek J., Owen F., 2006, arXiv:astro-ph/0612111v1
Feretti L., 2003, in: Bowyer S., Hwang C.-Y. eds., Matter and Energy in Clusters of Galaxies
Ferrando P. et al., arXiv:astro-ph/0508674
Fusco-Femiano R., 2004, Ap&SS, 294, 37
Govoni Feretti L., 2004, IJMPD, 13, 1549
Giovannini M., 2004, Int. J. Mod. Phys., D13, 391-502
Inoue S. et al., 2005, ApJ, 628, L9
Jungman G. et al., 1996, Phys. Rep., 267, 195
Marchegiani P., Perola G. C., Colafrancesco S., 2007, A&A, 465, 41
McNamara B. R., Nulsen P. E. J., 2007, arXiv:0709.2152
Peterson J. R., Fabian A. C., 2006, Phys. Rep. in press, astro-ph/0512549
Pfrommer C. et al., 2007, arXiv:0707.1707
Ryu D. et al., 2003. arXiv:astro-ph/0305164
Sanders J. C., Fabian A. C., 2007, arXiv:0705.2712
Sarazin C. L., 2001, arXiv:astro-ph/0105418
Seljak U. et al., 2006, Phys. Rev. Lett. 97, 191303,
Sigl G. et al., arXiv:astro-ph/0409098
Shaposhnikov M., 2007, arXiv:astro-ph/0703673
Springel V. et al., 2005, arXiv:astro-ph/0504097
Sunyaev R., Zel'dovich Ya. B., 1980, ARAA, 190, 413
Viel M. et al., Phys. Rev. Lett. 97, 071301
Yuksel H. et al., 2007 (arXiv:0706.4084v1)
Watson C. R. et al., 2006, Phys. Rev. D 74, 033009
Wolfe B., Melia F., 2006, ApJ, 638, 125